Design and fabrication of 3D-printed planar Fresnel zone plate lens

PLEASE CITE THE PUBLISHED VERSION

http://dx.doi.org/10.1049/el.2016.0736

PUBLISHER

IET

VERSION

VoR (Version of Record)

Design and fabrication of 3D-printed planar Fresnel zone plate lens

S. Zhang✉

3D-printing has been used for rapidly prototyping a low-cost and light-weight dielectric Fresnel zone plate lens. This lens was comprised of four dielectric zones and they were fabricated in one process with the tailored permittivities. Measurements show that this lens provides 7.3–12.8 dB gain enhancement over the frequency band from 8 to 12 GHz.

Introduction: Fresnel zone plate lenses (FZPLs) are relatively thin and light weight compared with conventional shaped lenses, which make them suitable for various consumer antenna applications [1–3]. The lens surface can be grooved to change wave phase velocity to achieve focusing effects [4]. Another method to accomplish the phase correction is to divide the lens into several concentric zones with different dielectric constants. This approach can be either realised by several tightly fitted concentric dielectric rings with various dielectric constants or perforating a uniform dielectric material to create different dielectric zones [5, 6]. These traditional fabrication approaches are dominated by using precise machining, and tight tolerances are required particularly for high-frequency applications. Sometimes cracking may happen in the materials during the perforating process. This increases manufacturing costs and complexity.

The advanced 3D-printing technology provides a simple alternative approach to fabricate the dielectric FZPL in one single process with minimal labour time and low material cost. Furthermore, while the machining technique removes parts of the raw materials and generates material waste, the 3D-printing is an additive manufacture process which minimises the material waste.

3D-printed dielectric materials: The tightly fitted concentric dielectric zones in the FZPL can all be 3D-printed using one single 3D-printing material. By altering the volume fractions of the air voids in the 3D-printed dielectrics, the dielectric constants can be tailored to the desired values. For rapid prototyping, the required volume fraction f of a non-solid 3D-printed dielectric can be expressed by (1), which shows the relation between the relative permittivity of the 3D-printing material ε_{ro} and the expected relative effective permittivity of the non-solid structure $\varepsilon_{\text{reff}}$

$$f = \frac{\varepsilon_{\text{reff}} - 1}{\varepsilon_{ro} - 1} \qquad (1)$$

In this Letter, the FZPL was 3D-printed by using a fused deposition modelling (FDM) Makerbot® Replicator™ 2X. Traditional 3D-printing filaments for FDM printing such as polylactic acid and acrylonitrile butadiene styrene (ABS) generally have a relative permittivity below 3. Low relative permittivity materials result in a thicker lens which increases the weight. PREPERM® TP20280 is a 3D-printing filament that is specially designed for RF applications. It is a composite ABS-based mixture with sub-micron scale dielectric additives which increase its relative permittivity to 4.4. The loss tangent of this filament is 0.004. For best printing results from the FDM 3D-printer, the extrusion temperature of the Replicator™ 2X was 230°C and the heated platform was 120°C.

Lens design and fabrication: The design of the FZPL was carried out at 10 GHz and the lens had a uniform thickness for a flat profile. The radii (Ri) for each dielectric zone can be determined using (2)

$$R_i = \sqrt{2Fi\left(\frac{\lambda_o}{P}\right) + \left(i\frac{\lambda_o}{P}\right)^2}, \quad i = 2,\ 3,\ \ldots,\ P \qquad (2)$$

where P is the phase correcting index, λ_o is the design wavelength and F is the focal length. In this Letter, the lens was designed for quarter wave phase correction and had $P = 4$. An F/D ratio of 0.3 was chosen, to obtain a short focal length, where D was the diameter of the FZPL. The focal length F was 30 mm.

The thickness of the lens t is related to the permittivities of two adjacent Fresnel zones and it can be obtained using (3)

$$t = \frac{\lambda_o}{P\left(\sqrt{\varepsilon_{ri}} - \sqrt{\varepsilon_{ri-1}}\right)}, \quad i = 2,\ 3,\ \ldots,\ P \qquad (3)$$

In this design, the highest relative permittivity value is 4.4 which is the 3D-printing material. To reduce the thickness and the weight, the centre ring with the minimum permittivity is equal to 1 which means an air ring can be used.

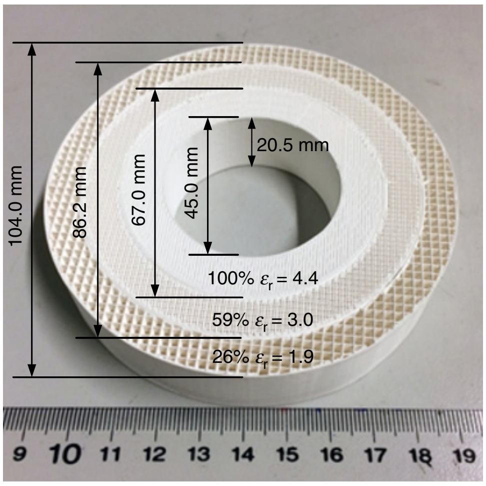

Fig. 1 *Photograph and geometry of 3D-printed FZPL*

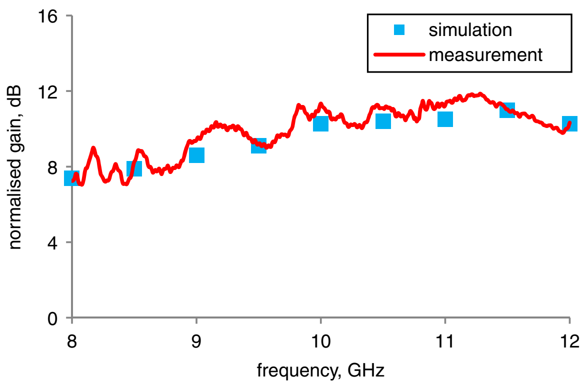

Fig. 2 *Normalised gain of 3D-printed FZPL*

By substituting $P = 4$, $t = 20.5$ mm, $\varepsilon_{\text{rmax}} = 4.4$, $\varepsilon_{\text{rmin}} = 1$ and $\lambda_o =$ 30 mm into (2), the required permittivities were obtained. It is worth noting that the FZPL has the lowest permittivity at the first Fresnel zone from the centre and the maximum at the second Fresnel zone. The other dielectric constant values then were decreased from the inner to the outermost. Therefore, the permittivities of the FZPL zones in this case had $\varepsilon_{r2} > \varepsilon_{r3} > \varepsilon_{r4} > \varepsilon_{r1}$.

The final 3D-printed dielectric FZPL is shown in Fig. 1. The infill of the second ring is 100% and the infill of the outermost ring is 26%. The whole lens was 3D-printed in a single process and the total fabrication time took ~3 h. The lens weighed 120.2 g.

Far-field measurement results: A far-field pattern scan experiment was set up for measuring the gain and the radiation patterns of the 3D-printed dielectric FZPL. This system scanned the received power over 180° in the azimuth-plane to generate the front half of the far-field radiation patterns. An X-band waveguide was placed at the focal point of the FZPL as the source. The distance between the waveguide and the lens was 30 mm which was the focal length of the FZPL. A horn antenna that measured the received power was placed at the same height of the waveguide and lens, and 1.5 m away. The horn antenna was mounted on a track and revolved half circle around the FZPL.

The normalised gain of the FZPL at the frequency band from 8 to 12 GHz is shown in Fig. 2. The gain value is the received power at boresight ($\theta = 0°$) with the lens normalised to the received power without the lens. This result indicates the gain enhancement of the 3D-printed FZPL. The simulated results using CST Microwave Studio is included in Fig. 2 for a comparison. In the simulation, the cylinder rings in the FZPL were solid without the air voids and were given the relative permittivities that were the same as shown in Fig. 1. The measured results agree well with the simulated results, and show that the 3D-printed FZPL increases the received power level by 7.3–12.8 dB over the entire 8–12 GHz range.

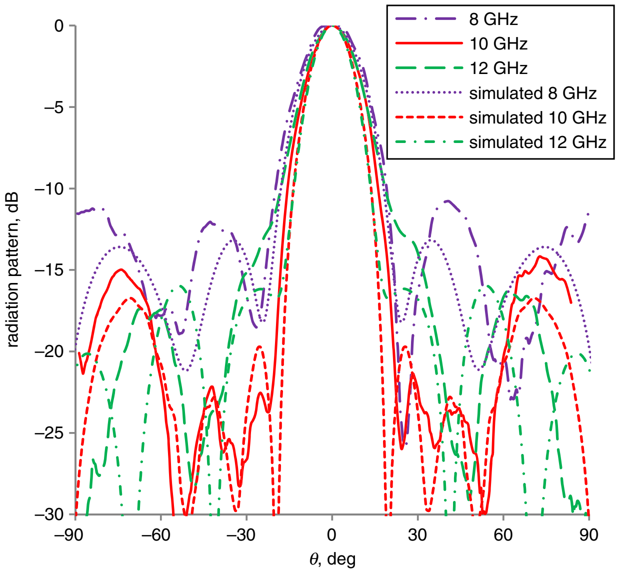

Fig. 3 *Far-field radiation patterns of 3D-printed FZPL in H-plane at different frequencies*

The measured far-field radiation patterns of the FZPL at 8, 10 and 12 GHz are shown in Fig. 3, and compared with the simulated patterns. The radiation patterns are normalised to the maximum received power at boresight at each individual frequency. Fig. 3 shows a good agreement between measurements and simulations. It can be observed that with the increased frequency the side lobe level is reduced. At the centre frequency 10 GHz, the −3 dB beamwidth of the FZPL was measured as ~18°. The first side lobe was ~15.2 dB lower than the main beam.

Conclusions: A low-profile, light-weight and wideband dielectric zone plate FZPL has been successfully rapidly prototyped using FDM 3D-printing. The entire lens was 3D-printed in a single-step process without machining or assembling, which significantly simplified the manufacturing process. The 10.4 cm diameter FZPL with quarter wave phase correction was comprised of three dielectric rings and one empty ring at the centre. These tightly fitted dielectric rings with the bespoke permittivities were 3D-printed as non-solid internal structures with specific material infill percentages. An equation has been derived to determine the infill percentages for 3D-printing the required effective relative permittivities of the non-solid structures. This 3D-printed dielectric FZPL offered 7.3–12.8 dB gain over the frequency range from 8 to 12 GHz, when fed by an X-band waveguide source that was located at the focal point of the lens.

Acknowledgments: This work was supported by the EPSRC Doctoral Prize Research Fellowship. The author thank the colleagues Dr. Will Whittow, Prof. Yiannis Vardaxoglou and Prof. Raj Mittra for valuable discussion concerning this work and thank Premix for providing the 3D-printing filament.

Submitted: *4 March 2016* E-first: *19 April 2016*
doi: 10.1049/el.2016.0736
One or more of the Figures in this Letter are available in colour online.

S. Zhang (*Wolfson School of Mechanical, Electrical and Manufacturing Engineering, Loughborough University, Loughborough LE11 3TU, United Kingdom*)

✉ E-mail: S.Zhang@lboro.ac.uk

References

1 Black, D.N., and Wiltse, J.C.: ‘Millimeter-wave characteristics of phase-correcting Fresnel zone plates’, *IEEE Trans. Microw. Theory Tech.*, 1987, **35**, (12), pp. 1122–1129, doi: 10.1109/TMTT.1987.1133826
2 Hristov, H.D., and Herben, M.H.A.J.: ‘Millimeter-wave Fresnel-zone plate lens and antenna’, *IEEE Trans. Microw. Theory Tech.*, 1995, **43**, (12), pp. 2779–2785, doi: 10.1109/22.475635
3 Hristov, H.D., and Rodriguez, J.M.: ‘Design equation for multidielectric Fresnel zone plate lens’, *IEEE Microw. Wirel. Compon. Lett.*, 2012, **22**, (11), pp. 574–576, doi: 10.1109/LMWC.2012.2224099
4 Wiltse, J.C.: ‘The Fresnel zone-plate lens’, *Millim. Wave Technol. III*, 1985, **544**, pp. 41–47, doi: 10.1117/12.948247
5 Petosa, A., and Ittipiboon, A.: ‘Design and performance of a perforated dielectric Fresnel lens’, *IEE Proc., Microw. Antennas Propag.*, 2003, **150**, (5), p. 309, doi: 10.1049/ip-map:20030267
6 Petosa, A., Ittipiboon, A., and Thirakoune, S.: ‘Investigation on arrays of perforated dielectric Fresnel lenses’, *IEE Proc., Microw. Antennas Propag.*, 2006, **153**, (3), p. 270, doi: 10.1049/ip-map:20050193